Monitoring System of a Large Rockslide in Heisei-Shinzan Lava Dome, Mt. Unzen, Japan

Yasuyuki HIRAKAWA[1*], Nobuhiro USUKI[1], Kouji FUJITA[1], Toshiaki TANAKA[1], Masafumi KANEKO[1], Toshiyasu UENO[2], Hidenori EGUCHI[2] and Kazuhiro SHIMOKUBO[2]

[1] Asia Air Survey Co., Ltd. (Shinyuri 21 Building, 1-2-2 Manpukuji, Asao-ku, Kawasaki City, 215-0004, Japan)
[2] Ministry of Land, Infrastructure, Transport and Tourism (2-1-3 Kasumigaseki, Chiyoda-ku, Tokyo, Japan)
*Corresponding author. E-mail: ys.hirakawa@ajiko.co.jp

It is concerned that a large rockslide is possible to occur at lobe 11 in Heisei-Shinzan lava dome, Mt. Unzen. Predicted collapse block of 10^7 m^3 was delimited based on geological structure and distribution of groundwater and superficial fractures. 6 types of in-situ and long-distance monitoring instruments have been installed. Surface of lobe 11 has moved to SE-ESE at rate of 2.45-5.77 cm/year in last decade, similar to other European rockslides or a little smaller. Results of the monitoring and other investigations indicate that creep deformation of subsurface pyorclastic-flow deposits induces slide and settlement of lobe 11, leading to toppling movement at the back-crack. For emergency managements, thresholds and evaluation procedure were established based on measurement. Threshold consists of three categories (i.e. "immediate", "short-term" and "long-term") according to length of lead time before the final collapse. A new index-value ISSV was adopted for threshold of seismometer. In the evaluation procedure, a flowchart using each instrument's status was prepared to mitigate either overestimation or underestimation.

Key words: Rockslide, Monitoring System, Monitoring Instrument, Threshold, Seismometer

1. INTRODUCTION

Landslides are one of the most frequent natural disasters. Especially, large rockslides such as Mayuyama in Japan, 1792 [*Inoue*, 1999] and Vajont in Italy, 1963 [*Kiersch*, 1965] have caused large human or economic loss.

In Mt. Unzen, southern Japan, a lava dome called "Heisei-Shinzan" was formed by eruptions during 1990-1995 [*Nakada et al.,* 1999]. An unstable rock mass named lobe 11 exists on east-side steep slope of the lava dome. It is concerned that a huge collapse and consequent debris avalanche are possible to occur, because lobe 11 has moved about 1.2-m downslope during last 20 years according to an observation by total station (hereafter TS) started in 1997 [*Hirakawa et al.*, 2017]. A result of numerical calculation showed debris avalanche would cause a severe damage to residential area, farmland and Route 57 and 521, located at 4-6 km downstream from lobe 11 in Shimabara city and Minami-Shimabara city [*Kondo et al.*, 2014]. Thus, as measures against the possible lava dome collapse, the Unzen Restoration Work Office of the Ministry of Land, Infrastructure, Transport and Tourism (hereafter MLIT) has been providing the non-structural measurements such as construction of monitoring system to minimize human loss, as well as the structural measurements to minimize damage in influenced area.

Several reports of monitoring large rockslides, including in-situ observations, have been presented in a few decades, mostly in Europe - e.g., Séchiliene in France [*Helmstetter and Grambois*, 2010], Runion in Italy [*Crosta and Agliardi*, 2002], La Saxe in Italy [*Manconi and Giordan*, 2014; *Manconi and Giordan*, 2015], Mannen in Norway [*Kristensen and Blikra*, 2013; *Blikra and Kristensen*, 2016] and Åknes in Norway [*Oppikofer et al.*, 2009]. However, their objects are not a lava dome like Mt. Unzen. On the other hand, in Japan, report of continuous measurement of large rockslide is rare, while mounts of slow-moving landslides on gentle slopes have been instrumented.

In this report, the authors introduce the integrated monitoring system constructed by MLIT, and then discuss the results of measurement and establishment of thresholds for huge collapse of lobe 11, Heisei-Shinzan lava dome.

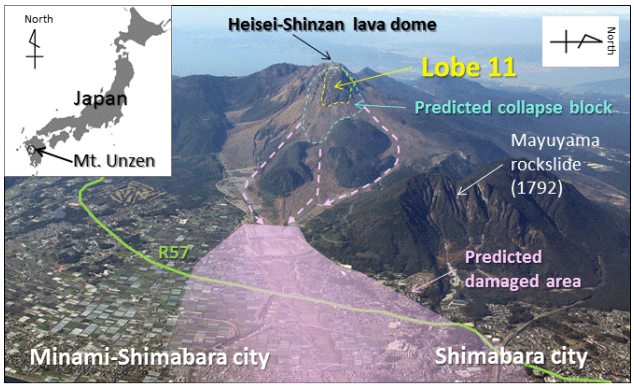

Fig. 1 Location and aerial view Mt. Unzen

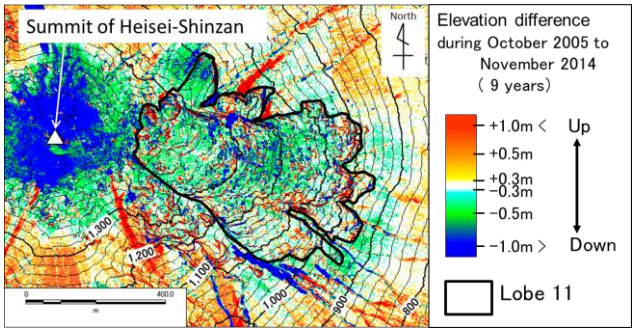

Fig. 2 Elevation difference calculated using LiDAR DTM

2. SITE DESCRIPTION

2.1 Forming process of lobe 11

Mt. Unzen is a volcano with 25km wide north-south which occupies most part of the Shimabara Peninsula, western Kyusyu region, southern Japan (shown in **Fig. 1**). The volcano consists of dozens of summits including Mt. Fugen.

A small eruption started at the summit of Mt. Fugen in November 1990, which was followed by thousands of pyroclastic-flow eruptions [*Nakada et al.,* 1999; *UI et al.*, 1999]. Since the eruption, lava lobes repeated growth and collapse. Lava blocks changed to pyroclastic flows as falling downslope and made large fan with pyroclastic-flow deposits. In total 13 lobes were appeared during May 1991 to March 1995, before Shimabara Earthquake and Volcano Observatory of Kyushu University (hereafter SEVO) stated the eruptive activity came to an end. Lobe 11 is located on east-side slope of the lava dome as an unstable, large rock mass with approximately 500m in width, 600m in length and 35-40 degrees in incline.

Data set obtained by TS measurement from 1997 revealed that surface of lobe 11 had moved downslope approximately 100 cm in 14 years [*Tamura and Maeda*, 2012]. Result of calculation using DTM from LiDAR showed that whole lobe 11 had been lowered around several dozen centimeters in 9 years (shown in **Fig. 2**). Field survey started at 2008 revealed that several rockfalls occurred every year at cliffs edge of lobe 11. These results inferred that slide and settlement are coinciding on whole lobe 11, which possibly lead to large rockslide in the future. Thus MLIT started construction of integrated monitoring system since 2011.

2.2 Delimitation of predicted collapse block

Preparing arrangement plan of monitoring instruments, delimitation of predicted collapse block is important. Although predicted breaking line on a longitudinal cross section was showed [*Kondo et al.*, 2014], the definite position of scarp or limit in transverse direction were not specific. Therefore we determined them based on results of investigation shown below.

DTMs, superficial geological maps and geological profiles on cross sections at 8 periods during 1991-2009 were provided by topographical and geological analysis using multi-temporal aerial photographs and sketch drawings during eruptions [*Watanabe et al.*, 2010]. They showed subsurface geological structure beneath the lava dome which consists of 3 lava lobes and pyroclastic-flow deposits (possibly including failure deposits) accumulated alternatingly above old ground surface that existed before 1990-1995 eruptions (hereafter "pre-eruption surface"), and planar and vertical distributions of the lobes. Coinciding of slide and settlement of lobe11 is considered to be caused by creep deformation of the pyroclastic-flow deposits, which have only past 26 years from their deposition and easy to be compressed and fractured by heavy rock mass of lava lobe.

On the other hand, we suggested a possibility that groundwater or high-moisture layer exists between pre-eruption surface and pyroclastic-flow deposits from studies of debris-flow causes on downslope of lobe 11 [*Hirakawa et al.*, 2015a; *Hirakawa et al.*, 2016]. It coincides with the results of airborne and field electromagnetic surveys [*Mantoku et al.*, 2013; *Ueno et al.*, 2017]. Furthermore, we presented detailed maps showing topographical features and ground cover (shown in **Fig. 3**) by interpreting DTM from LiDAR and hundreds of aerial photographs taken at close range in October 2014 [*Hirakawa et al.*, 2015b]. The maps disclosed cracks, gullies and fumarole areas which are possible to make boundary of collapse.

We predicted collapse block based on the results of investigation above, considering as follow [*Ueno et al.*, 2016]. Creep or slide would occur in vulnerable pyroclastic-flow deposits or at the

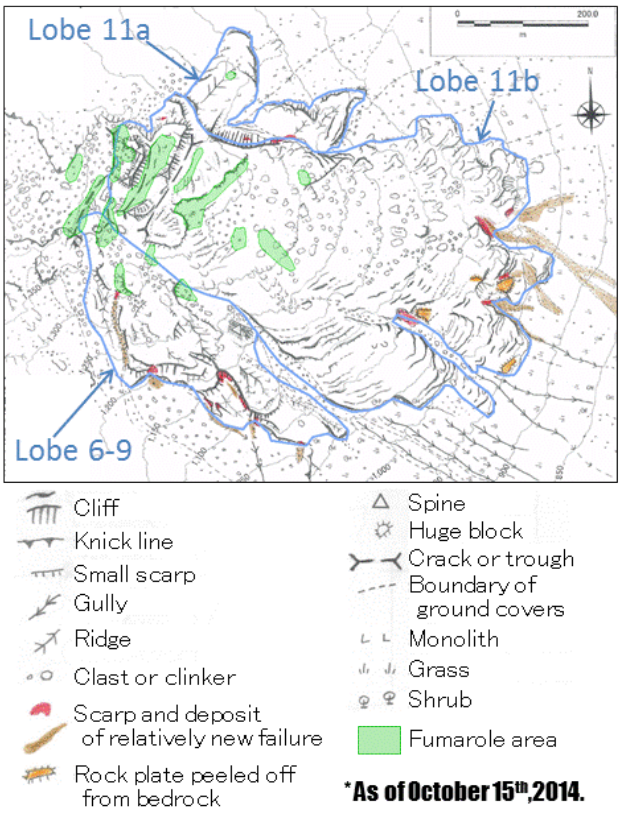

Fig. 3 Detailed map showing topographic features and groundcover of lobe 11

boundaries of them. Pyroclastic-flow deposits layer directly above the pre-eruption surface is particularly easy to be vulnerable because of pore water pressure or piping with existence of rich groundwater. Just under the right and left limit of lava lobes, shear fracture of pyroclastic-flow deposits would be caused by drastic change of upper load in transverse direction. Fumaroles and distinct cracks would make collapse boundary because clefts are likely continued to deep zone. Based on these ideas, we draw breaking lines of collapse on 3 longitudinal cross sections and 19 transverse ones (shown in **Fig. 4 and 5**), and then reflected them to planar map (shown in **Fig. 6**). As a result, four scenarios of collapse were predicted. Area and volume of the largest collapse was estimated as 70 ha and in order of 10^7 m^3, respectively.

3. MONITORING INSTRUMENTS AND METHODS

6 types of in-situ and long-distance monitoring instruments have been set on and around lobe11 as of September 2017 as shown in **Fig. 6, Fig. 7** and **Fig. 8**. Rain gauges and cameras are also installed by MLIT but not shown in the figures.

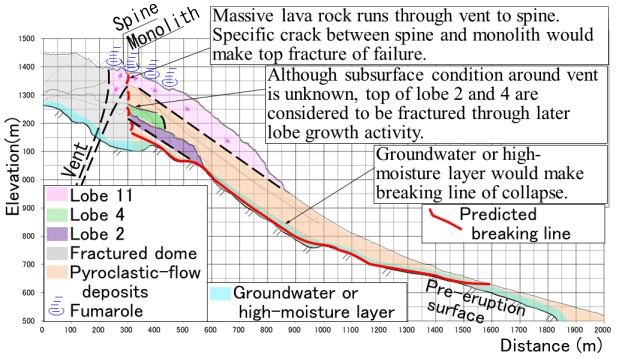

Fig. 4 Cross section corresponding to Line A

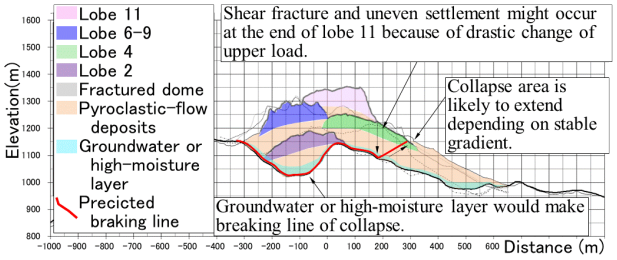

Fig. 5 Cross section corresponding to Line B

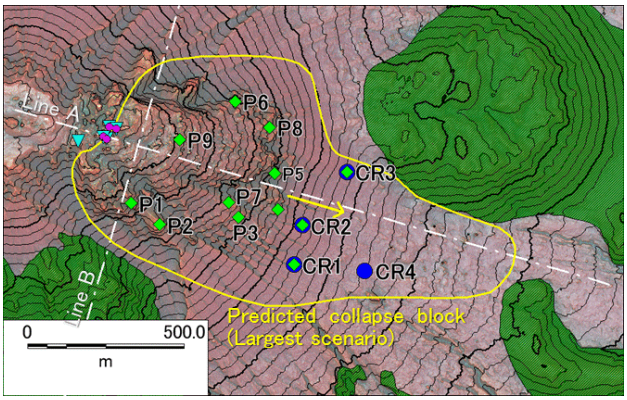

Fig. 6 Predicted collapse block and lines of cross sections. Instrumentation sites are also shown for the same legend as Fig. 7. Green shade shows pre-eruption surface

3.1 Total stations (TS)

Measuring distance between 2 TSs and 10 prisms on lobe 11 was started in March 1997 [*Tamura and Maeda*, 2012]. Because surface of lobe 11 is covered by spines and unstable blocks, transporting and setting prisms by hand was too risky and helicopter was used to transport 1-ton concrete blocks as the foundation of the prisms [*Nakazato et al.*, 2006]. While 10 prisms had been set at first, they got out of use except P7 and P8 because of volcanic gas, and were supplemented with new P1-6 prisms in May, 2006 [*Sawada et al.*, 2007]. After predicting collapse block, new 3 prisms (CR1-3) were added on downslope in July, 2016, and 1 prism (P9) on upper slope in the predicted collapse block in November, 2016. As of September 2017, 12 prisms are arranged in total. Distance between TSs

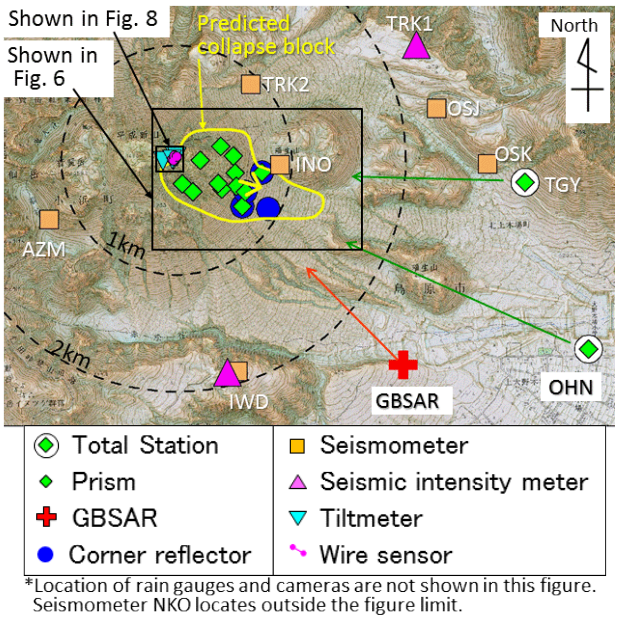

Fig. 7 Arrangement of monitoring instruments

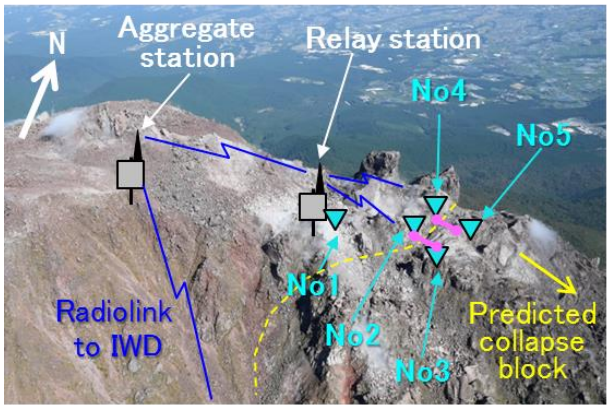

Fig. 8 Photograph of top of lobe 11. Location of tiltmeters and wire sensors are shown for the same legend as Fig. 7

and prisms are approximately 2-4 km. TSs were at first located approximately 1km away from OHN and TGY, but relocated in 2006.

Periodical and manual measurement was performed at first, but continuous automatic measurement with 1-hour time intervals was started in September, 2007 [*Tamura and Maeda*, 2012]. Data set of distance obtained every hour varies so widely that average value for 24 hours is usually used, but every hourly data is used to compare with "immediate" threshold which will be described later.

3.2 Ground-based SAR (GBSAR)

TS has disadvantage that it can measure distance only to the prisms (in other words point-based), and only in good weather conditions with no clouds and no fogs. To cover this disadvantage, Ground-Based Synthetic Aperture Rader (hereafter GBSAR) started measurement in October 2011 [*Tamura and Maeda*, 2012]. However, reflected radar intensity from downslope of lobe 11 was poor due to dense growth of bushes and grasses. Thus 4 corner reflectors were set in July 2016, although it is point-based measurement same as TS.

Displacement is analyzed using two data sets measured at different times. While data is acquired every 7 minutes, analyzing interval was set to two days to distinguish actual displacement from atmospheric effects [*Satou et al.*, 2014]. However, displacement of every 7 minutes is analyzed for comparison with "immediate" threshold which will be described later.

3.3 Seismometers and seismic intensity meters

Though several seismometers are installed on and around the lava dome, in this paper, we only refer to those installed by MLIT.

Seismometers were installed to detect pyroclastic flows or debris flows at first, but they started being treated as useful instruments to detect rockfalls through the discussion about monitoring system for large rockslide. The oldest of them were installed at IWD which contains 2 types of seismometer (described later), and started measurement in April 1994 [*Miki et al.*, 1998]. Although 2 more seismometers were set at the same time at other sites, they were moved to OSJ and OSK in 2005. Other seismometers were installed at NKO in 2005, INO and TRK2 in 2007, AZM in 2016. As of September 2017, 8 seismometers are arranged on 7 sites in total.

Short-period vertical sensor corresponding to frequencies of 1-20 Hz was installed at each site, and in addition also broadband 3-component sensor responding to 0.008-50 Hz was installed at IWD. All of them are velocity sensors and have sampling rate of 100 Hz. Acquired data is sent to MLIT by wire except particular sections using radio-link from INO and TRK2 to wired antennas.

Two seismic intensity meters started measurement in May 2017 to detect the outbreak of the earthquake that may become the inducement of the large collapse.

3.4 Tiltmeters and wire sensors

Five tiltmeters and 2 wire sensors were set on and around the top of the predicted collapse block in December, 2016 (shown in **Fig. 8**). It was a very hard mission to set the instruments because of severe weather conditions, inaccessible rock cliffs, and farness from electric power supply and telecommunications infrastructure. However, since grasping the behavior of the upper area of the block is essential for the monitoring of whole rockslide,

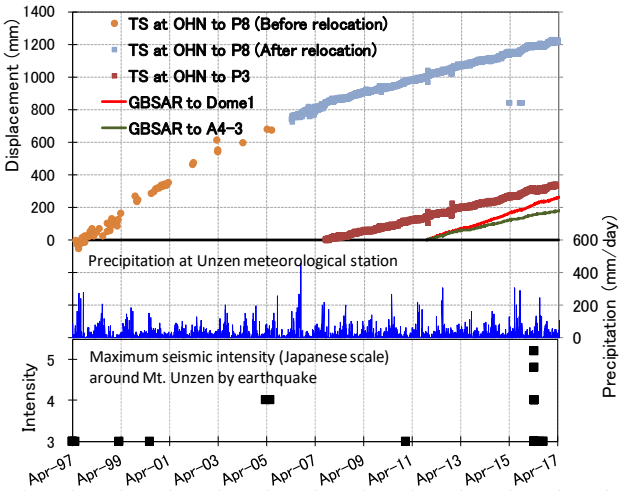

Fig. 9 Surface displacement measured by TS and GBSAR. Precipitation and seismic intensity of earthquake by Japan Meteorological Agency are also shown

we overcame the hardness and completed the setting of instruments. The mission was made possible by making system configuration which includes state-of-the-art power-saved tiltmeters, solar batteries and wireless installations, and taking 3 flights of helicopter for 700 kg material handling and 8 times field work.

Tiltmeter consists of three-axis acceleration sensors so that tilt fluctuation of each axis is calculated. Data is sent to IWD using radio-link. Though measuring time interval of tiltmeter is set to 24 hours to save power, it can be changed shorter by remote control in emergencies.

4. RESULTS OF OBSERVATION

4.1 Surface displacement

Sample of the observation result of the surface displacement is shown in **Fig. 9**. Displacement of P8 seems to decelerate around 2005, which probably indicate transition from the first creep phase to the second creep phase, though conclusion is not easy because the TS was relocated at the same period. Total displacement of P8 is 1.26 m in 20 years since May 1997, corresponding to 6.2 cm/year. After automatic observation of P1-P8 began in September 2007, their displacement rates are 2.45-5.77 cm/year, which differ depending on sites of TSs and prisms. Moving directions of P1-P8 are analyzed to SE-ESE from two displacement rates of different TS sites [*Satou et al.*, 2014].

Spatial distribution of total displacement by GBSAR in a year is shown in **Fig. 10**. Terrain sheds and low-reflection zones are shown in gray color. The largest displacement is exhibited in "Dome1" area located at knick line, while larger and smaller

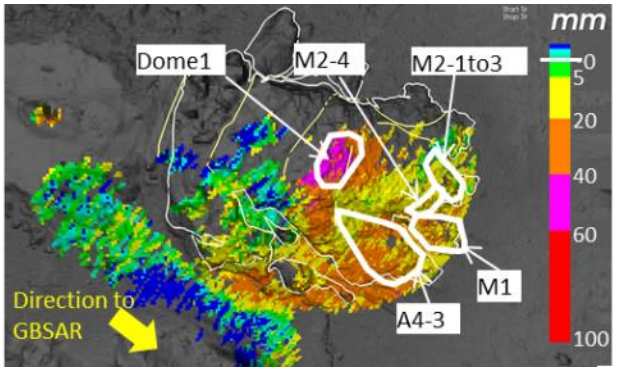

Fig. 10 Spatial distribution of total displacement measured by GBSAR from March 1st, 2016 to February 28, 2017

displacement zones are distributed complexly in other area. Although the distribution likely reflects subsurface geological structures, interpretation is difficult, because tendency of distribution is more complicated than mention in past documents [*Tamura and Maeda*, 2012; *Satou et al.*, 2014]. Five areas shown in **Fig. 10** (e. g. "Dome1" and "M2-4" and so on) are monitoring subjects for comparison with thresholds.

Displacement rates by GBSAR at "Dome1" and "A4-3" area are substantially constant, 4.8cm/year and 3.3cm/year respectively, during October 2011 and February 2017 (shown in **Fig. 9**). TS's measurement of P3 prism located within "A4-3" area indicate 3.6 cm/year displacement rate, which is consistent with GBSAR's measurement.

As for new sites P9 and CR1-4, observation periods are too short to estimate long term trend, but displacement rate P9 is faster and CR1-4 are slower than the other prisms.

4.2 Seismic signals and seismic intensity

From 2004 to 2016, every seismogram was automatically stored only when one or more sensor detected amplitude larger than 3.5 millikine (kine means cm/s) with duration longer than 10 seconds. Number of the records is 80 - 538 per a year. It is thought that the amplitude relatively larger among them is caused by rockfalls, failures, debris flows, earthquakes and noises. Representative of them is shown in **Fig. 11**.

In case of rockfalls and failures, duration tends to be several seconds or several tens of seconds including rapid increase and decrease of amplitude. However, failures of relatively larger magnitude can exhibit seismograms similar to debris flow with duration of several minutes. In case of debris flow, the seismogram exhibits long duration of several minutes to few hours with fusiform envelope featured by gentle increase and decrease. Some seismograms of debris flows include impulsive

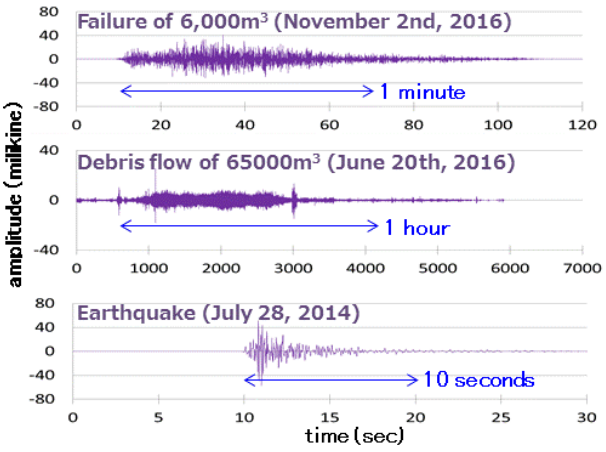

Fig. 11 Different types of seismograms measured at INO

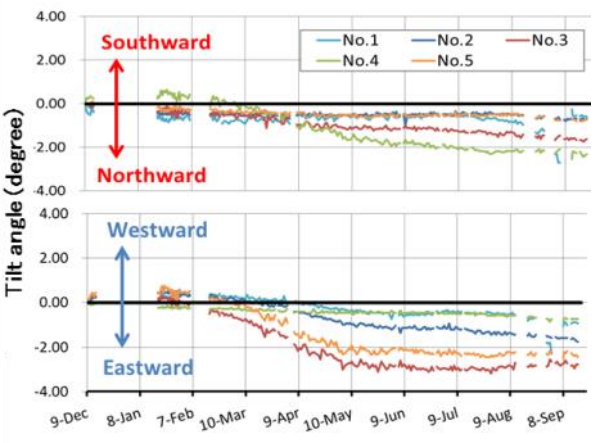

Fig. 12 Tilt fluctuation at the top of lobe 11 from tiltmeter in 9 months from the end of 2016

signals, which are probably caused by bank failures in debris flow. In case of earthquake, all sensors provide similar seismograms at almost the same time, which are featured by rapid increase followed by gradual attenuation.

Results of seismic intensity measurement are consistent with announcement of Japan Meteorological Agency and results of seismometer measurements.

4.3 Tilt fluctuation at the top of lobe 11

Time series of measurement by tiltmeters are shown in **Fig. 12**. Although the data before middle of February 2017 lack by system error, after that, data has been stored successfully. Generally all sensors exhibit northward and eastward fluctuation. Especially No.3 and No.5 exhibit the largest fluctuations eastward among all sensors during March and May, and No.2 follows. Comparing this fact with the location of each sensor (see **Fig. 8**), it is indicated that toppling deformation is evolving at the top of the predicted collapse block. However,

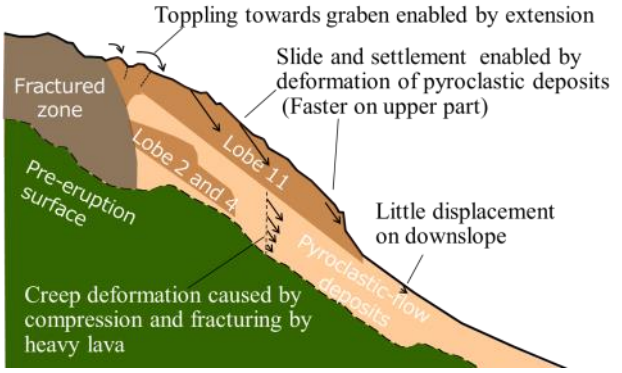

Fig. 13 Schematic profile across lobe 11 rockslide

there is a possibility that it is only seasonal fluctuation influenced by external factors such as temperature. At least a year measurement will be needed for initial calibration.

4.4 Interpretation and instability mechanisms

Based on results of investigations and observations above, instability mechanisms are considered as below (shown in **Fig. 13**). Primary factor of instability is considered to be creep deformation of pyroclastic-flow deposits caused by compression and fracturing by upper load of heavy rock mass of lava lobe. It induces slide and settlement of lobe 11 as measured by TSs, GBSAR and LiDAR. The reason why displacement is faster on upper part is possibly related to subsurface geological structure. Toppling deformation on the top of lobe 11 is possible to infer opening of back-crack depending on slide movement.

5. ESTABLISHING THRESHOLDS

5.1 Approach

Debris avalanche following large collapse of lobe 11 is estimated to reach Route 57 and residential area in approximately 5 minutes. Therefore the information about occurrence of large collapse or precursory phenomena is needed to be provided to decision makers for emergency managements.

Useful methods for this purpose are, for instance, comparing measured data with thresholds established previously, or forecasting time of failure. *Crosta and Agliardi* [2002] proposed a method to define different values of threshold velocities corresponding to time before failure, by developing an equation between velocity and acceleration under power-law creep movement [*Voight*, 1988]. *Manconi and Giordan* [2014, 2015] presented straightforward statistical method to forecast time of failure in near-real-time, using time

Table 1 Summary of thresholds. "TW" means reference time-window

Instru-ment	Cate-gory	Index-value and threshold
Seismic intensity meter	Imme-diate	**Intensity >= 4** (on the Japanese scale) Measured at TRK1 or IWD
Seismo-meter	Imme-diate	**1) ISSV >= 10^5 milikine^2 *s or** **2) [Duration with amplitude >= 40milikine] >= 30s** Measured at more than 1 site among INO, TRK2, IWD and AZM
TS	Imme-diate	**Velocity >= 20mm/h** (TW= 1h) Measured at more than 1 combination of arbitrary 1 prism and both of 2 TS's
	Short-term	**Difference from regression line >= 4cm or successive twice 2cm** (Regression line of TW= 100days)
	Long-term	**Velocity >= 0.3mm/day** (TW= 100days)
GBSAR	Imme-diate	**Velocity >= 4mm/h twice consecutively** (TW= 1h)
	Short-tem	**Velocity >= 1.45mm/day** (TW= 2 days)
	Long-term	**Velocity >= 5cm/year** (TW= 1 year)
Wire sensor	Imme-diate	Cut of both of 2 sensors

series of inverse-velocity. However, these methods are useful in tertiary creep stage when displacement exhibits acceleration. Lobe 11 at Mt. Unzen is considered to be in second creep stage when displacement rate is constant (shown in **Fig. 9**), which not allow to apply these methods. Hence we established thresholds for each instrument corresponding to the maximum level of deviation of index-value calculated from past observation. It is a rather traditional but available method as of now.

5.2 Categories of thresholds

We established three categories of thresholds (i.e. "immediate", "short-term" and "long-term") according to length of lead time before the final collapse. "Immediate" thresholds were set to detect inducement, premonitory phenomena (e.g. rapid increase of rockfalls or acceleration) or final large-scale collapse. "Short-term" and "long-term" thresholds were set to find change of coefficient of creep curve. Among the thresholds, the "immediate" is most important because it might be applied to evacuation order for residence, and because "short-term" and "long-term" are not useful in case of sudden collapse by a heavy external force (e.g. earthquake) with no tertiary creep curve previous. Thresholds we established are summarized in **Table 1**. Among them, the thresholds for TS, GBSAR and seismometer are taken up below.

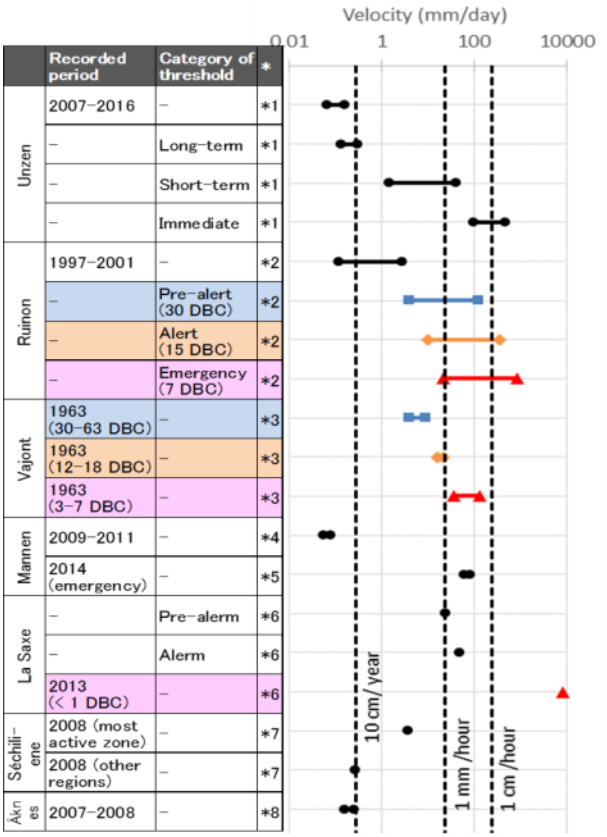

*References
*1: This paper
*2: *Crosta and Agliardi* [2002]
*3: Read from a graph shown in *Voight* [1988]
*4: *Kristensen and Blikra* [2013]
*5: *Blikra and Kristensen* [2016]
*6: *Manconi and Giordan* [2014]
*7: *Helmstetter and Garambois* [2010]
*8: *Oppikofer et al.* [2009]

Fig. 14 Velocities recorded or set as thresholds. "DBC" means "Days before Collapse"

5.3 TS and GBSAR

"Long-term" thresholds are aimed at detecting gentle acceleration of long-term displacement rate (velocity), which possibly indicates start of tertiary creep phase. Index-values of TS and GBSAR were set to velocities in reference time-windows of 100 days and 1 year respectively, because seasonal deviation is large in short time-windows. "Short-term" and "immediate" thresholds are aimed at detecting relatively swift and significantly rapid acceleration, respectively. Index-values are velocities in time-windows shorter than "long-term".

Velocities recorded in the past or set as thresholds in 7 rockslides are shown in **Fig. 14**. Red, orange and blue colors indicate days before collapse of less than 10 days, 10-20 days and 30-70 days, respectively. The monitoring subjects are in the order of 10^6 - 10^8 m^3, though actually collapsed or active blocks are a portion of them except Vajont.

As shown in **Fig. 14**, the recent velocity and "long-term" threshold of Mt. Unzen is on the same level as other rockslides in normal state or a little smaller. When increase of the "long-term" threshold will be needed because of frequent excess of measured data in the future, **Fig. 14** will be useful as reference.

On the other hand, “immediate” threshold is not smaller than alert (orange color) and emergency (red color) level in other rockslides. Note that it is larger than the velocity at 3 days before huge collapse of 200 million m^3 at Vajont. The “immediate” threshold velocity is so large because reference time-window was set to short time aiming at detecting rapid acceleration in near-real-time, and because velocity in short time-window exhibit wide-range deviation. In case real velocity including no measurement error exceeds the threshold, circumstances might be very risky.

5.4 Seismometer

Seismometers as well as wire sensors take important places as real-time measuring instrument. Two index-values were set for thresholds of seismometer. One is "Integrated value of Square of Seismic Velocity (hereafter ISSV)", a new index-value we propose, which indicates the increase of rockfalls, failures or fracture openings leading to final collapse. Another is combination of amplitude and duration.

5.4.1 ISSV

It is known that rockfalls or partial failures occur as precursory phenomena of rockslides. Observing the records of past rockslides, both frequency and volume of rockfall seem to increase with time. In that cases, it is considered that counting number of collapse blocks or estimating volume of each block is very difficult because seismic signals caused by some rockfalls and subsequent avalanches would overlap within durations. But detecting increase of seismic energy generated by hitting of rock blocks is possible. According to literatures, collapse volume of lava dome was proportional to the tremor energy calculated from linear envelope manually drawn on seismogram of pyroclastic flow during 1991 eruption at Mt. Unzen [*Takarada et al.*, 1993]. Volume of debris flow was strongly correlated with time-integrated amplitude of seismic acceleration [*Suwa et al.,* 1999].

We defined ISSV at time of t_0 which indicates seismic energy by Eq. (1):

$$ISSV = \int_0^{T_w} v_{t_0-t}{}^2 dt \qquad (1)$$

where v_t is the seismic velocity at time of t and

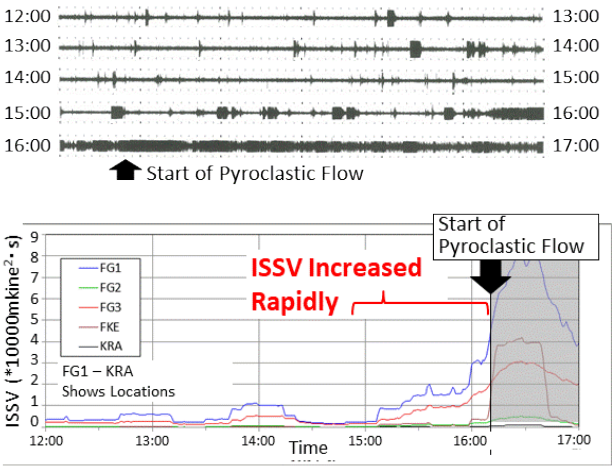

Fig. 15 Seismograms (upper) and time series of ISSVs (lower) before a pyroclastic flow at June 3rd, 1991

T_w is reference time-window. Time series of ISSVs with different T_w were calculated using seismic signals measured by SEVO at two pyroclastic flows in the order of 10^5-10^6 m^3 on June 3rd and 8th, 1991. The results showed ISSVs increased rapidly just before occurrence of pyroclastic flow in case T_w is around 30-120 minutes (case of 30 minutes is shown in **Fig. 15**). Compared to seismogram, it is understood that increase of ISSV is associated with increase of intermittent large waveforms since about 15:00 followed by sequential wave since about 15:50. These seismic waves are possibly induced by rockfalls, partial failures or micro-earthquakes caused by fracture openings, considering that 99% of pyroclastic flows during 1990-1995 eruptions were triggered by partial collapse of lava dome [*Nakada et al.,* 1999] and that rockfalls are frequently observed before rockslides. Moreover, larger amplitude than sensor's range seems to have occurred from the waveform in the seismogram. If it had been recorded, ISSV value would exhibit more rapid increase. Hence we adopted ISSV for an index-value which can detect precursory phenomena, for “immediate” threshold. Because we set the ISSV values using current seismometers location, the defined threshold (10^5 millikine^2 *s) is different from **Fig. 15**.

5.4.2 Amplitude and duration

We adopted combination of amplitude and duration of seismic wave for the index-value to detect final large-scale collapse. Based on past measurement, relatively larger amplitude is considered to be caused by rockfalls, failures, debris flows or earthquakes except noises. Because large-scale collapse would induce much larger amplitude than rockfalls, failures and debris flows past recorded, amplitude threshold (40 millikine)

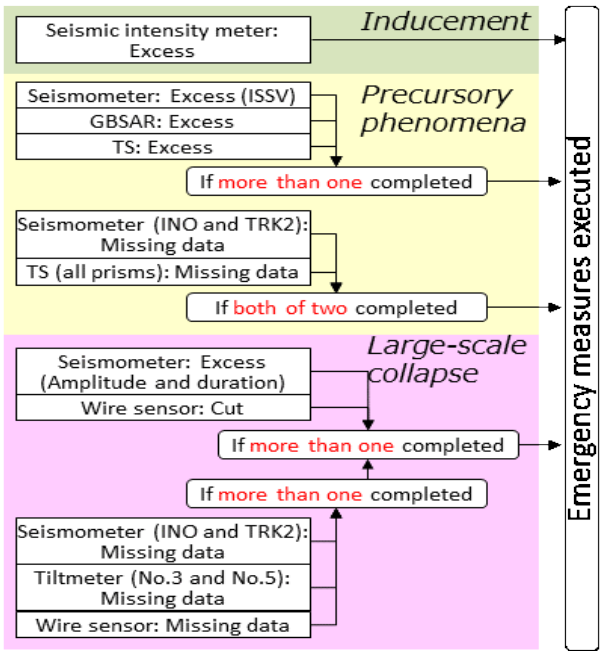

Fig. 16 Evaluation flowchart for "immediate" thresholds

was set to larger level than maximum value of them. On the other hand, seismic wave of earthquakes frequently exceed 40 millikine, but most of them end quickly so that duration threshold was set to 30s. Exceeding the threshold at more than one site is required to avoid overestimation. In two years since setting threshold, that condition occurred 19 times during the 2016 Kumamoto Earthquakes (Mw 7.0), but only 2 times at other earthquakes.

6. EVALUATION PROSEDURE

We set two steps of evaluation because of wide variety of monitoring instruments. In the first step, measurement by each instrument is compared with the thresholds. And in the second step, condition is evaluated based on combination of the excesses. As for "long-term" and "short-term" thresholds, corresponding actions will be executed simply when data set of one type of instrument exceed the threshold. In contrast, evaluation for "immediate" thresholds must be performed carefully because it might be applied to evacuation order for residence. Hence a flowchart was prepared to judge whether emergency measures should be executed (shown in **Fig. 16**).

In the flowchart, we paid attention to mitigate either overestimation or underestimation. To avoid overestimation, necessary condition was set to cases in which measurement records exceed the thresholds for more than one type of monitoring instruments. To avoid underestimation, we regarded missing data of multiple instruments as indicator of occurrence of precursory phenomena or final large-scale collapse, because instruments and prisms on or near lobe 11 are easy to get useless by destruction, disappearance, or loss of radio directivity in case of large displacement or frequent rockfalls.

Condition corresponding to emergency measures has never occurred in six months, since April 2017, after the new warning system incorporating the thresholds and the flowchart was installed.

7. CONCLUSIONS

MLIT has been providing structural and non-structural measurements against large rockslide in Heisei-Shinzan lava dome, Mt. Unzen. This report shows delimitation of predicted collapse block, methods and results of monitoring, establishment of the thresholds and evaluation procedure based on combination of the thresholds. Recent displacement rate of lobe 11 was on the same level to other European rockslides or a little smaller. A new index-value ISSV calculated from seismic signals was proposed for detecting precursory phenomena. Future issues will be maintenance of instruments, initial calibration of newly installed instruments, to verify the thresholds based on accumulated data and to discuss definite action when thresholds will be exceeded.

ACKNOWLEDGMENT: We wish to appreciate Dr. E. Shimokawa, Dr. H. Shimizu, Dr. Y. Jiang and Dr. T. Yamada for helpful constructive suggestions and discussions. We also thank Dr. K. Umakoshi and H. Takeishi for analyzing seismic data, and K. Yoshikawa and T. Shibata for making available GBSAR and TS data. Instrumentation at top of the lobe 11 could not been possible without the help from many engineers including K. Tada and T. Toyoshima. Finally, we thank Dr. H. Bateer, Dr. W. Yagi and an anonymous reviewer who helped improve the manuscript and the English.

REFERENCES

Blikra, L. H. and Kristensen, L. (2016): Monitoring a rockslide in development, INTERPRAEVENT 2016, extended abstracts, pp.158-159.

Crosta, G. and Agliardi, F. (2002): How to obtain alert thresholds for large rockslides, *Physics and Chemistry of the Earth*, Vol. 27, pp.1557-1565.

Helmstetter, A. and Garambois, S. (2010): Seismic monitoring of Séchilenne rockslide (French Alps): Analysis of seismic signals and their correlation with rainfalls, *JGR*, Vol. 115, F03016.

Hirakawa, Y., Okano, K., Tanaka, M., Takeishi, H., Sato, Y., Metoko, J. and Okamoto, T. (2015a): Relationship between

sediment movement and topographical and geological factor at Mizunashi river, Mt. Unzen, Proc. 64th Annual Congress of JSECE, B, pp.54-55 (in Japanese).

Hirakawa, Y., Fujita, K., Tanaka, M., Usuki, N., Chiba, T., Satoh, Y., Metoko, J. and Okamoto, T. (2015b): Detailed interpretation of topography and ground cover at lobe 11, Mt.Unzen, Proc. 64th Annual Congress of JSECE, B, pp. 432-433 (in Japanese).

Hirakawa, Y., Okano, K., Takeishi, H., Ueno, T. and Mitsutake H. (2016): Occurence condition of debrisflow at Mizunashi river, Mt. Unzen, Proc. 65th Annual Congress of JSECE, JSECE Publication No.78, B, pp. 252-253 (in Japanese).

Hirakawa, Y., Usuki, N., Fujita, K., Tanaka, T., Kaneko, M., Ueno, T., Eguchi, H. and Shimokubo, K. (2017): Monitoring system for a large collapse of Heisei-Shinzan, Mt. Unzen, Proc. 66th Annual Congress of JSECE, JSECE Publication No. 81, pp.598-599 (in Japanese).

Inoue, K. (1999): Shimabara-Shigatusaku earthquake and topographic changes by Shimabara catastrophe in 1792, *J. of JSECE*, Vol. 52, No. 4, pp. 45-54 (in Japanese with English abstract).

Kiersch, G. A. (1965): The Vaiont Reservoir Disaster, Mineral Information Service, Vol.18, No. 7, pp. 129–138.

Kondo, R., Anyoji, N., Fujisawa, Y. and Sato, Y. (2014): Evaluation of potential hazards from lava dome collapse on Mt. Unzen-Fugen-Dake, INTERPRAEVENT 2014, Vol. 1, pp. 84-91.

Kristensen, L. and Blikra, L. H. (2013): Monitoring displacement on the Mannen rockslide in western Norway, C. Margottini et al. (eds.), Landslide Science and Practice, Vol. 2, pp.251-256.

Manconi, A. and Giordan, D. (2014): Landslide failure forecast in near-real-time, *Geomatics, Natural Hazards and Risk*, Vol. 7, pp.639-648.

Manconi, A. and Giordan, D. (2015): Landslide early warning based on failure forecast models: the example of the Mt. de la Saxe rockslide, northern Italy, *NHESS*, Vol. 15, pp. 1639-1644.

Mantoku, M., Sugiyama, M., Todaka, T., Yuuki, Y., Kuroki, M., Ohuchi, H., Sakurai, K. and Kawahara, Y. (2013): Analysis of subsurface structure of Mt. Unzen based on airborne electromagnetic survey, Proc. 62th Annual Congress of JSECE, A, pp. 118-119 (in Japanese).

Miki, Y., Igarashi, S., Itoh, H. and Ozeki, N. (1998): Analysis of seismic waveform by debris flow in Mt. Fugen, Unzen, Proc. 47th Annual Congress of JSECE, pp.322-323 (in Japanese).

Nakada, S., Shimizu, H. and Ohta,K. (1999): Overview of the 1990–1995 eruption at Unzen Volcano, *JVGR*, Vol. 89, pp. 1-22.

Nakazato, K., Matsui, M., Yamaguchi, K., Hata, K. and Ohbayashi, K. (2006): Development of emergency observation system for a large-scale slope, Proc. 55th Annual Congress of JSECE, pp. 138-139 (in Japanese).

Oppikofer, T., Jaboyedoff, M., Blikra, L., Derron, M.-H. and Metzer, R. (2009): Characterization and monitoring of the Åknes rockslide using terrestrial laser scanning, *NHESS*, Vol. 9, pp. 1003-1019.

Satou, Y., Ishizuka, T., Kuraoka, S., Nakashima, Y. and Kmijo, T. (2014): Deformation characteristics of Unzen lava dome based on long range displacement monitoring, INTERPRAEVENT 2014, Vol. 1, pp.92-100.

Sawada, E., Matsui, M., Yamaguchi, K., Hata, K., Ishitsubo, S. and Mizuta, T. (2007): Study of lava dome's behavior using target prism at Mt. Fugen, Unzen volcano, Proc. 56th Annual Congress of JSECE, pp. 234-235 (in Japanese).

Suwa, H., Yamakoshi, T. and Sato, K. (1999): Estimation of debris-flow discharge by monitoring ground tremor, *J. of JSECE*, Vol. 52, No. 2, pp. 5-13 (in Japanese with English abstract).

Takarada, S., Kazahaya, K., Kawanabe, Y., Sakaguchi, K., Sudo, S., Yamamoto, T., Soya, T. and Unzendake Weaher Station, JMA (1993): Volume estimation of 1991-92 eruption of Unzen Volcano, and initiation mechanisms of pyroclastic flows on June 3 and June 8, 1991, *Bull. Geol. Surv. Japan*, Vol. 44, No. 1, pp.11-24 (in Japanese with English abstract).

Tamura, K. and Maeda, A. (2012): Monitoring of lava dome of Unzen volcano by EDM and ground based synthetic aperture radar, *J. of JSECE*, Vol. 65, No. 1, pp. 69-72 (in Japanese).

Ueno, T., Mitsutake, H., Fujita, K., Usuki, N. and Hirakawa, Y. (2016): Dilimiting predicted collapse blocks based on topographical development process of lava dome, Mt. Unzen, Proc. 65th Annual Congress of JSECE, JSECE Publication No. 78, B, pp.400-401 (in Japanese).

Ueno, T., Mitsutake, H., Shimokubo, K., Miki, Y., Ohuchi, H., Kitahara, T., Uehara, Y., Sakurai, K. and Todokoro, H. (2017): Estimating subsurface structure and mechanisms of large collapse based on airborne and field electromagnetic survey at Heisei-Shinzan lava dome, Mt. Fugen, Proc. 66th Annual Congress of JSECE, JSECE Publication No.81, pp. 66-67 (in Japanese).

Ui, T., Matsuwo, N., Sumita, M. and Fujinawa, A. (1999): Generation of block-and-ash flows during the 1990–1995 eruption of Unzen Volcano, Japan, *JVGR*, Vol. 89, pp. 123–137.

Voight, B. (1988): A method for prediction of volcanic eruptions, *Nature*, Vol. 332, pp. 125-130.

Watanabe, F., Maeda A., Takaba, E., Matsuo, Y., Sakka, S., Hasegawa, R., Nakamura, T. and Yamaguchi, S. (2010): Estimating subsurface structure of a lava dome at Mt. Fugen, Unzen volcano, Proc. 59th Annual Congress of JSECE, pp. 338-339 (in Japanese).